Journal of Alloys and Compounds, 191 (1993) 43–49
JALCOM 442

Thermodynamic calculations in quaternary transition metal systems

Hai Wang, Reinhard Lück and Bruno Predel
Max-Planck-Institut für Metallforschung, Institut für Werkstoffwissenschaft, and Institut für Metallkunde der Universität Stuttgart, Seestraße 75, W 7000 Stuttgart 1 (Germany)

(Received 25 July, 1992)

Abstract

A new geometry of interpolation has been developed for computation of mixing properties in quaternary systems. The enthalpy and the Gibbs free energy of mixing are calculated by means of this geometry for intersections in quaternary Fe–Ni–Ti–Zr, Fe–Co–Ti–Zr and Ni–Co–Ti–Zr systems, of which corresponding properties in binaries are known. The spinodal decompositions in these systems are estimated. The critical temperatures of the miscibility gaps are calculated and the temperatures of the spinodal decompositions are represented by projections of three-dimensional figures.

1. Introduction

In previous papers [1, 2] we have carried out thermodynamic investigations on ternary systems, in which mixing enthalpies of liquid ternary alloys are calculated by using different geometries of interpolation and the results of the computation are compared with the experimental results. The best suitable geometry, which is used to interpolate the thermodynamic properties within the whole composition range of ternary systems, was determined by comparison with experimental data.

The prediction of the thermodynamic properties of quaternary alloys from the corresponding properties of its binary boundary systems is often requested. In this paper we want to introduce a new geometry for the interpolation of thermodynamic properties of mixing in quaternary systems for particular combinations of components. By means of this geometry the mixing properties of quaternary Fe–Ni–Ti–Zr, Fe–Co–Ti–Zr and Ni–Co–Ti–Zr systems will be calculated.

According to the regular solution model, the miscibility gap usually appears when the mixing enthalpy is positive. That is true for binary alloys, but not necessarily for ternary systems. Meijering [3, 4] has reported how to calculate the miscibility gap on the basis of the known parameters of interaction of the binaries. It is really possible that the ternary alloys exhibit miscibility gaps, although their binaries have negative values of mixing enthalpies.

It is also of interest to determine the necessary conditions for the existence of a miscibility gap in quaternary systems.

The mixing enthalpies of liquid binary Fe–Ti [5], Co–Ti [6], Ni–Ti [7], Fe–Zr [8], Co–Zr [9], Ni–Zr [10], Fe–Ni, Fe–Co, and Ni–Co [11] alloys have been directly determined by calorimetric measurements. Kaufman and Bernstein [12] have calculated the enthalpy of mixing of liquid Ti–Zr alloys. Thus the enthalpies of mixing of all boundary binaries of the quaternary Fe–Ni–Ti–Zr, Fe–Co–Ti–Zr and Ni–Co–Ti–Zr systems are now available.

We came to the conclusion that these quaternary systems can be regarded approximately as reciprocal salt systems. Reciprocal salt systems are known for the formation of miscibility gaps in the liquid state. Therefore we tested the thermodynamic functions to determine whether miscibility gaps in the quaternaries are possible. If these do not exist in the liquid state but in supercooled liquids, important information is gained for the formation of amorphous alloys. Alloys of most of the binary boundary systems can be transformed to the amorphous state by rapid quenching and by other methods. Therefore the formation of two-phase amorphous alloys in the quaternaries considered here would be possible.

2. Geometry of interpolation

A quaternary system contains four components: A, B, C, D. If isobaric conditions are assumed, the graphical representation of the constitution of a quaternary system requires the representation of four variables: X_A, X_B, X_C and T. The most common system of coordinates used is the equilateral tetrahedron in which the apices

0925-8388/93/$6.00

represent the pure components, the edges represent the six binary systems, the triangular faces represent the four ternary systems, and finally the interior of the tetrahedron represents the quaternary system.

In principle, there are several possibilities for representing quaternary concentrations of components in the tetrahedron. One of them is given by the lines parallel to the edges of the binaries drawn through a concentration point in the tetrahedron. It is evident that the sum of concentrations of four components is equal to unity by means of this representation.

Mixing properties of liquid quaternary alloys are functions of three variables for isothermic conditions, from which it follows that the thermodynamic functions of quaternary alloys cannot be represented in three-dimensional figures. Therefore we emphasize our calculation on sections of the quaternary system. Hence, the number of variables is reduced to two for isothermic conditions. For these sections, it is possible to visualize the thermodynamic functions of quaternary alloys in a three-dimensional figure.

A special section is selected for the quaternary Fe–Ni–Ti–Zr, Fe–Co–Ti–Zr and Ni–Co–Ti–Zr systems, which is shown in Fig. 1 by the bold lines. In Fig. 1 the symbol A indicates the pure component iron or nickel; B represents the pure component titanium and C the pure component zirconium, and D stands for the component nickel or cobalt. The section shown in Fig. 1 is of importance because the enthalpies of mixing of liquid binary A–D and B–C (Ti–Zr, Fe–Ni, Fe–Co and Ni–Co) alloys have small absolute values. On the contrary, the binaries A–B, A–C, B–D and D–C (Fe–Ti, Ni–Ti, Co–Ti, Fe–Zr, Ni–Zr, Co–Zr) have large negative values of mixing enthalpies. As shown in Fig. 2, this section may be represented by four points: A_mB_{1-m}, D_mB_{1-m}, D_mC_{1-m} and A_mC_{1-m}, where m is a constant and $0 \leqslant m \leqslant 1$. The compositions of the four components at this section have the following relationship:

$$X_A + X_D = m \tag{1}$$

$$X_B + X_C = 1 - m \tag{2}$$

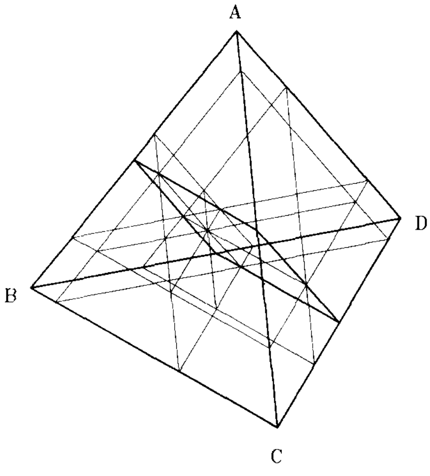

Fig. 1. The equilateral tetrahedron. The geometry of interpolation is indicated by the rectangular intersection.

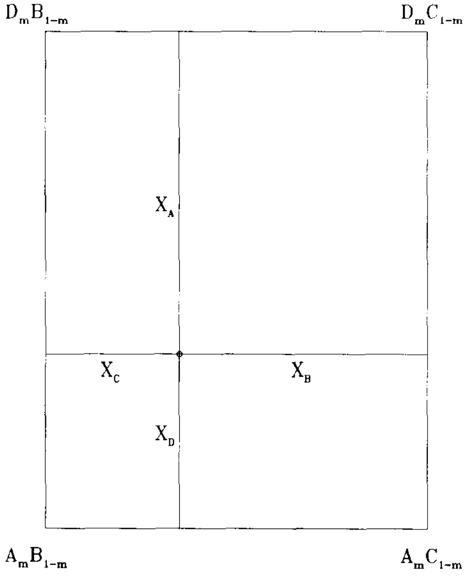

Fig. 2. The section selected in Fig. 1. The concentration of the quaternary alloy is marked and the four reference binary concentrations are given by the corners.

At this section (Fig. 1) the sums of the concentrations of A plus D and those of B plus C are constant. If m is taken as 0.5, this section is a square. The geometry chosen in this paper results in boundary ternary geometries of the type Toop, Hillert1 or Hillert2. Since we obtained the best results using these geometries in the ternaries, we have chosen this kind of generalization [1, 2]. The binary boundary concentrations taken as a basis for the interpolation are therefore chosen as $X_i^{i\text{-}j} = m$ and $X_j^{i\text{-}j} = 1\text{-}m$ in the four systems with strong interaction. These concentrations are given by the section of the indicated rectangular area with the binaries (Fig. 1) and represented in Fig. 2 by the four corners of the rectangle.

3. Algorithm of interpolation

The starting point of the calculation is based on the regular solution model. The following calculations are limited to the section shown in Figs. 1 and 2. In order to simplify the algorithm, we use 1, 2, 3, 4 instead of the symbols A, B, C, D to describe the four pure components. The mixing enthalpies of liquid quaternary alloys are given by

$$\Delta H = \frac{1}{2} \sum_i^4 \sum_j^4 C_{ij} X_i X_j \tag{3}$$

where i, j indicate the components of the mixture and $i, j = 1, 2, 3, 4$. C_{ij} is the interaction parameter of the liquid binary i–j alloys. X_i represents the mole fraction of the component i in the quaternary system.

To gain the algorithm of interpolation, the interaction parameters should be calculated first. The enthalpy of mixing of binary alloys is given by

$$\Delta H_{i-j} = C_{i,j} X_i^{i-j} X_j^{i-j} \tag{4}$$

where ΔH_{i-j} is the enthalpy of mixing of the binary i–j system. X_i^{i-j} and X_j^{i-j} are the reference mole fractions of the components i and j at the binary i–j edge. It is evident that X_i^{i-j} has a different meaning from X_i. The relationship between X_i^{i-j} and X_i is determined by the geometrical construction of the section represented in Figs. 1 and 2.

The quaternary Fe–Ni–Ti–Zr, Fe–Co–Ti–Zr and Ni–Co–Ti–Zr systems are supposed to correspond to the geometry of the so-called reciprocal salt systems, which are characterized by a strong interaction between the anions and cations. The interactions of early titanium, zirconium and late iron, cobalt, nickel transition metals are analogous to those of salts. The geometry of reciprocal salt systems is illustrated in Fig. 1 by A and D as anions and B and C as cations. Even though the quaternary systems considered here cannot be taken as a real reciprocal salt system, the large absolute values of mixing enthalpies in the binary systems justify this treatment.

For the binaries A–D and B–C different geometries can be used to obtain satisfactory results; even the asymmetric left-Colinet geometry [13] could be used:

$$C_{i,j} X_i X_j = \frac{X_i}{1 - X_j} \Delta H_{i-j}(X_i^{i-j} = X_i) \tag{5}$$

For the binary A–B, A–C, B–D and C–D systems the interaction parameters are given by

$$C_{i,j} = \frac{\Delta H_{i-j}(X_i^{i-j} = X_{\mathrm{A}} + X_{\mathrm{D}},\ X_j^{i-j} = X_{\mathrm{B}} + X_{\mathrm{C}})}{(X_{\mathrm{A}} + X_{\mathrm{D}})(X_{\mathrm{B}} + X_{\mathrm{C}})} \tag{6}$$

All interaction parameters C_{ij} can be calculated from eqns. (5) and (6). Therefore the mixing enthalpies of quaternary systems can be calculated from eqn. (3).

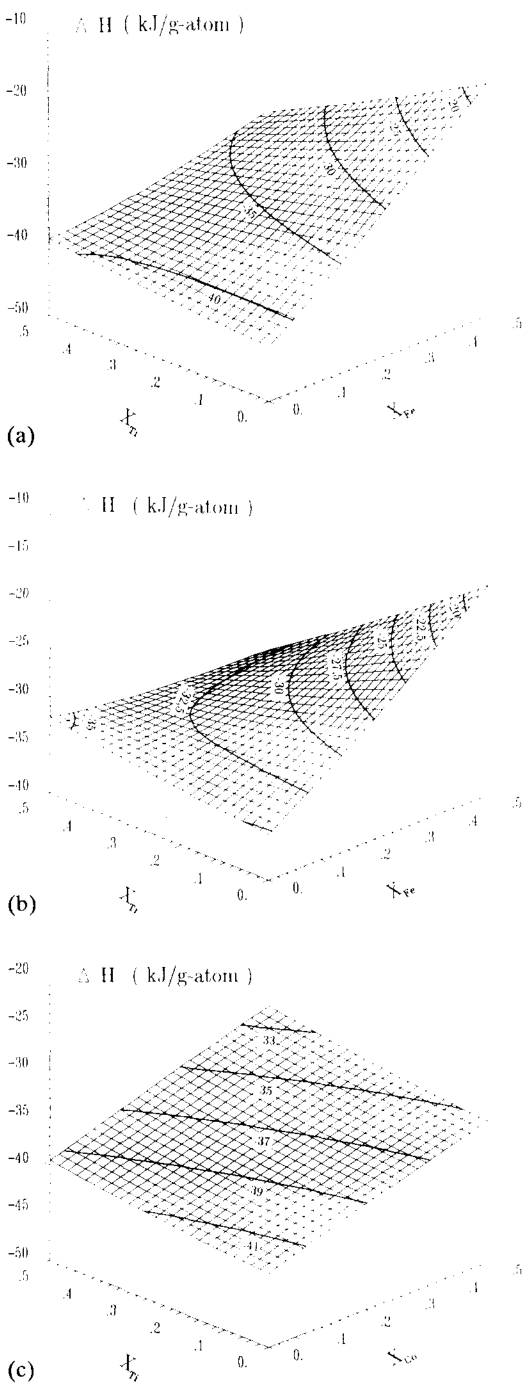

Fig. 3. Mixing enthalpy of liquid quaternary alloys at 1873 K for the section $m = 0.5$: (a) Fe–Ni–Ti–Zr; (b) Fe–Co–Ti–Zr; (c) Ni–Co–Ti–Zr.

4. Enthalpy and Gibbs free energy of mixing

Mixing enthalpies of liquid Fe–Ni–Ti–Zr, Fe–Co–Ti–Zr and Ni–Co–Ti–Zr alloys are calculated by the algorithm of interpolation developed as above. They are shown in Fig. 3. The mixing enthalpies of all quaternaries are calculated for the temperature 1873 K. The mixing enthalpies of liquid Ti–Zr alloys are calculated by means of the regular model. The concentration dependences of other binaries are described by a power series, the so-called thermodynamic adopted power (TAP) series [14]. The adjustable parameters used in the TAP series are listed in Table 1. It has to be pointed out that the mixing enthalpies of liquid binary alloys are not measured at the same temperature. For this reason, all mixing enthalpies considered here are assumed to be independent of temperature.

TABLE 1. Mixing enthalpies of liquid binary alloys

System	Enthalpy of mixing (kJ mol^{-1})
Fe–Ti	$\Delta H=(1-X_{Ti})(-57.3X_{Ti}-30.5X_{Ti}^2)$
Co–Ti	$\Delta H=(1-X_{Ti})(-100.5X_{Ti}-80.8X_{Ti}^2)$
Ni–Ti	$\Delta H=(1-X_{Ti})(-219.5X_{Ti}+100.8X_{Ti}^2)$
Fe–Zr	$\Delta H=(1-X_{Zr})(-89.7X_{Zr}-92.4X_{Zr}^2)$
Co–Zr	$\Delta H=(1-X_{Zr})(-145.0X_{Zr}+33.3X_{Zr}^2)$
Ni–Zr	$\Delta H=(1-X_{Zr})(-285.5X_{Zr}+255.1X_{Zr}^2)$
Fe–Ni	$\Delta H=(1-X_{Ni})(-7.1X_{Ni}-23.3X_{Ni}^2)$
Fe–Co	$\Delta H=(1-X_{Co})(-7.2X_{Co}-3.9X_{Co}^2)$
Co–Ni	$\Delta H=(1-X_{Ni})(1.64X_{Ni}-0.16X_{Ni}^2)$
Ti–Zr	$\Delta H=-5.4X_{Zr}X_{Ti}$

The following calculation of the Gibbs free energy of mixing is based on the assumption that the entropies of mixing of liquid quaternary alloys could be calculated by the model of the ideal solution. The Gibbs free energy of mixing of liquid quaternary alloys is then described by

$$\Delta G=\frac{1}{2}\sum_{i}^{4}\sum_{j}^{4}C_{ij}X_iX_j+RT\sum_{i}^{4}X_i\ln X_i \qquad (7)$$

Figure 4 shows the Gibbs free energies of mixing of liquid quaternary Fe–Ni–Ti–Zr, Fe–Co–Ti–Zr and Ni–Co–Ti–Zr alloys for the temperatures 1873 K. The Gibbs free energies of mixing represented in Fig. 4 are calculated for the section $m=0.5$. The bold lines in Fig. 4 are contour lines. It can be seen that there is a minimum of the Gibbs free energy of mixing for all quaternary alloys. The minimum is neither in the centre nor in the corner of the section $m=0.5$.

The Gibbs free energies of mixing of liquid Fe–Ni–Ti–Zr alloys at different temperatures are illustrated in Fig. 5 for the section $m=0.5$. Comparison of Fig. 4(a) and Fig. 5 makes it obvious that the concentration of the minimum changes with temperature. The minimum is shifted towards the boundary of the section with decreasing temperature because of the small entropy of mixing at low temperatures.

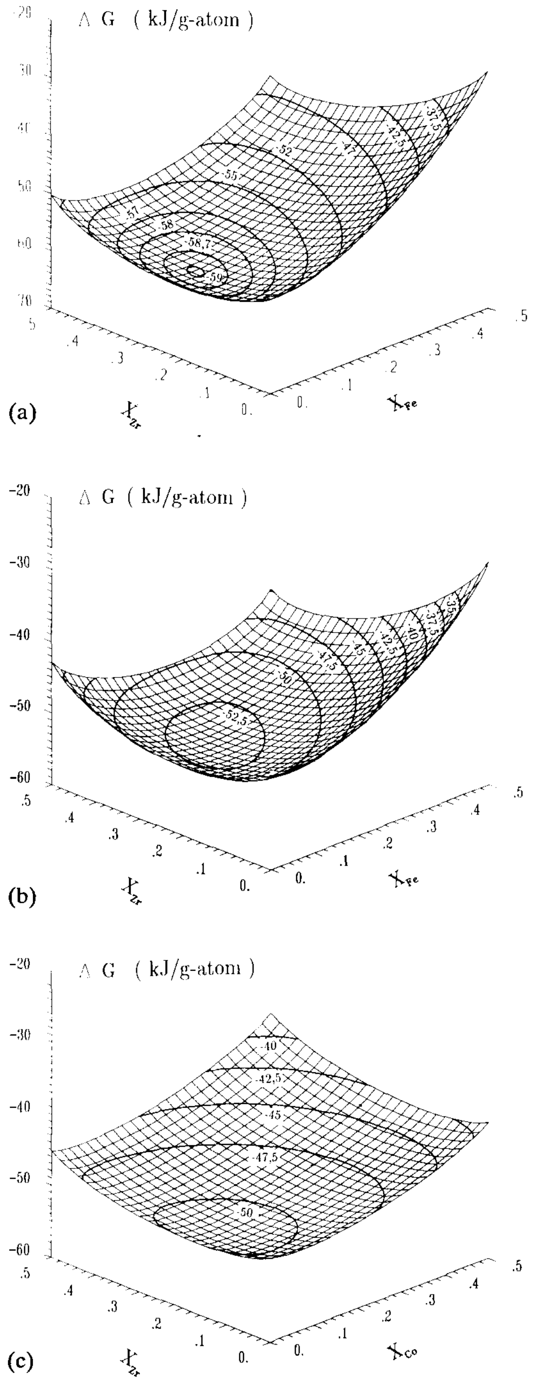

Fig. 4. Gibbs free energy of mixing of quaternary liquid alloys at 1873 K for the section $m=0.5$: (a) Fe–Ni–Ti–Zr; (b) Fe–Co–Ti–Zr; (c) Ni–Co–Ti–Zr.

5. Spinodal decomposition

The Gibbs free energy of quaternary alloys based on the regular model is given by

$$G=\sum_{i=1}^{4}X_iG_i^\circ+\frac{1}{2}\sum_{i=1}^{4}\sum_{j=1}^{4}C_{ij}X_iX_j+RT\sum_{i=1}^{4}X_i\ln X_i \qquad (8)$$

where G_i° indicates the Gibbs free energy of the pure components. G_i° is a function of temperature. Since

$$X_1+X_2=m,\ X_3+X_4=1-m$$

the Gibbs free energy G is only a function of the mole fractions X_1, X_3 and the temperature T. For isothermic conditions, the Gibbs free energy for the section shown in Fig. 1 can be represented as a function of X_1 and X_3 in a three-dimensional figure.

The problem of the determination of miscibility gaps is the question of how to gain the double-tangent planes at the surface given by eqn. (8). If the surface given by eqn. (8) is everywhere convex from below, no double-tangent plains are possible.

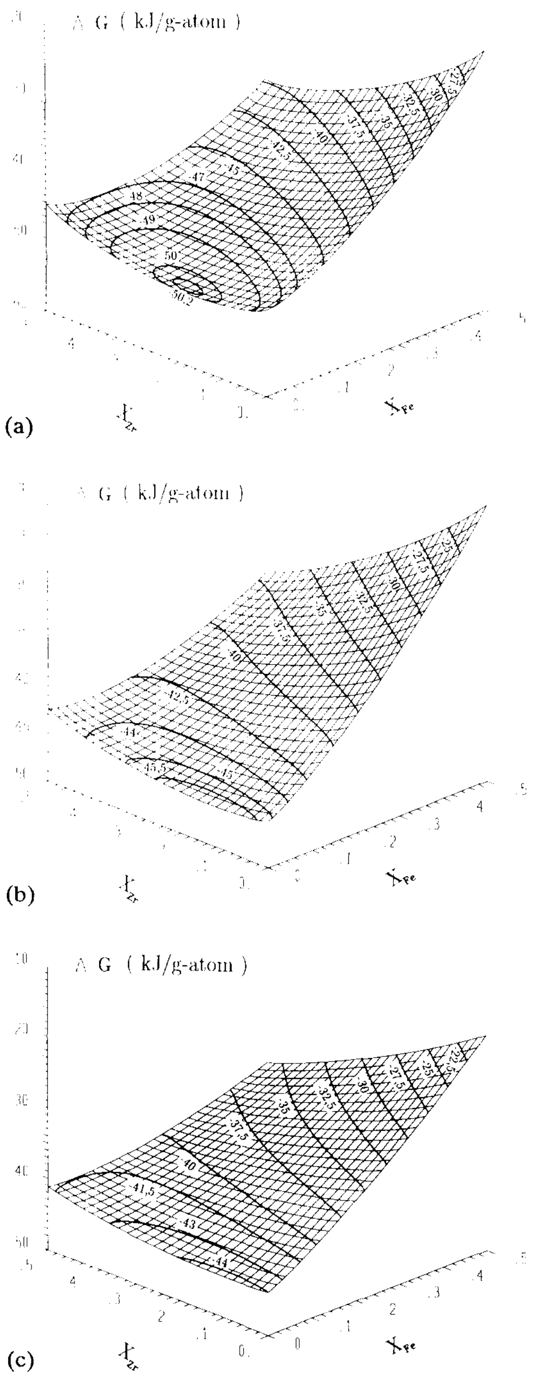

Fig. 5. Gibbs free energy of mixing of liquid Fe–Ni–Ti–Zr alloys for the section $m=0.5$: (a) 1000 K; (b) 500 K; (c) 298 K.

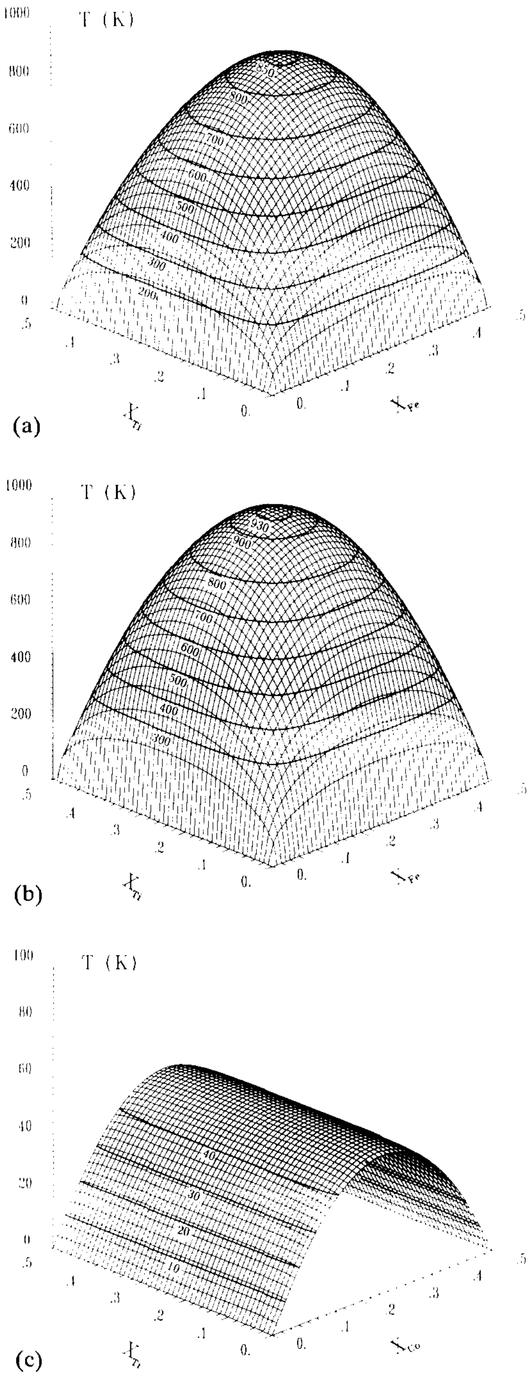

Fig. 6. Temperatures of the spinodal decomposition in quaternary systems for the section $m=0.5$: (a) Fe–Ni–Ti–Zr; (b) Fe–Co–Ti–Zr; (c) Ni–Co–Ti–Zr.

The second derivatives of the G function with respect to X_1 and X_3 are

$$\frac{\partial^2 G}{\partial X_1^2} = -2C_{12} + RT\left(\frac{1}{X_1} + \frac{1}{X_2}\right) \tag{9}$$

$$\frac{\partial^2 G}{\partial X_3^2} = -2C_{34} + RT\left(\frac{1}{X_3} + \frac{1}{X_4}\right) \tag{10}$$

$$\frac{\partial^2 G}{\partial X_1\,\partial X_3} = C_{13} - C_{23} - C_{14} + C_{24} \tag{11}$$

To determine the full convexity of the G function at a certain point (X_1, X_3) in the three-dimensional representation, a further second differentiation of the G function in an arbitrary direction is needed. In a direction V determined by $\mathrm{d}X_3/\mathrm{d}X_1 = n$, the curvature of the G function is given by

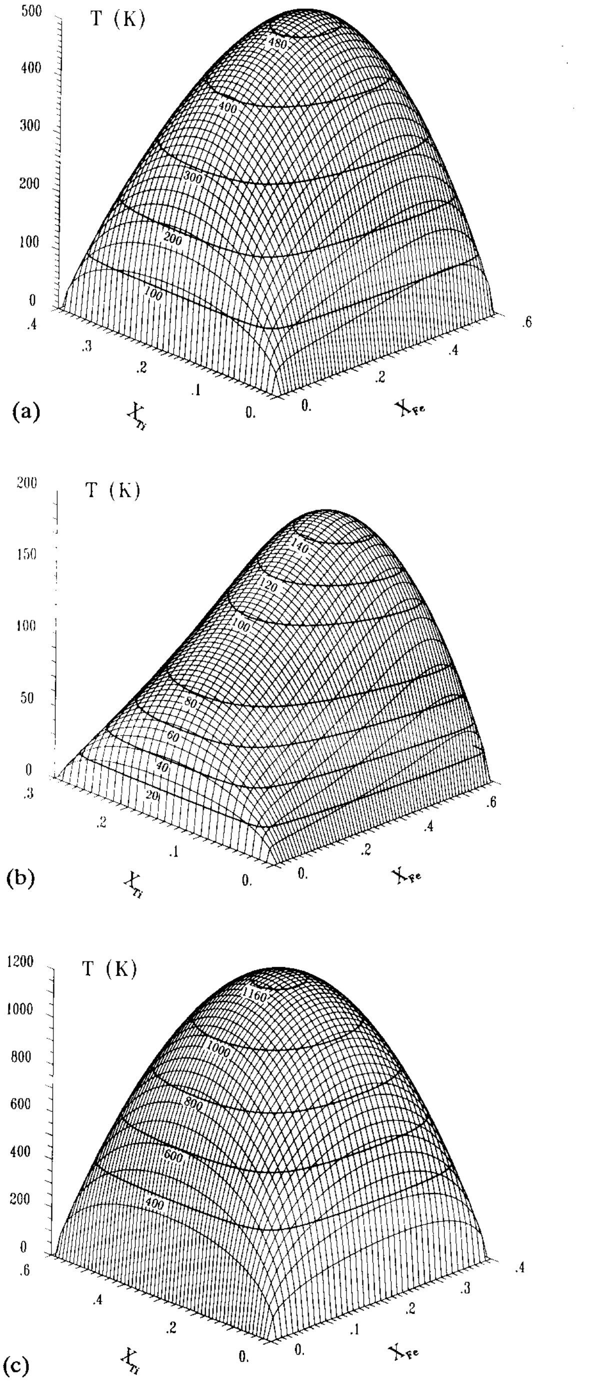

Fig. 7. Temperatures of the spinodal decomposition in the Fe–Ni–Ti–Zr system: (a) section $m = 0.6$; (b) section $m = 0.7$; (c) section $m = 0.4$.

$$\frac{\partial^2 G}{\partial V^2} = \frac{1}{1+n^2}\frac{\partial^2 G}{\partial X_1^2} + \frac{2n}{1+n^2}\frac{\partial^2 G}{\partial X_1\,\partial X_3} + \frac{n^2}{1+n^2}\frac{\partial^2 G}{\partial X_3^2} \qquad (12)$$

After a simple alteration of eqn. (12), the right-hand side becomes a power series of second order in n. If

$$\frac{\partial^2 G}{\partial X_3^2} > 0 \qquad (13)$$

$$\left(\frac{\partial^2 G}{\partial X_1\,\partial X_3}\right)^2 < \frac{\partial^2 G}{\partial X_1^2}\frac{\partial^2 G}{\partial X_3^2} \qquad (14)$$

$\partial^2 G/\partial V^2$ is always positive. If the second differentiation of the G function in an arbitrary direction V is positive, it is impossible that the G function has two different points which can be connected by a common tangent. That is, spinodal segregation does not exist in this case. If

$$\left(\frac{\partial^2 G}{\partial X_1\,\partial X_3}\right)^2 = \frac{\partial^2 G}{\partial X_1^2}\frac{\partial^2 G}{\partial X_3^2} \qquad (15)$$

there is only one direction at which $\partial^2 G/\partial V^2 = 0$. That indicates also that eqn. (12) has merely one reasonable solution. The direction V can therefore be determined from

$$n = -\frac{\partial^2 G/\partial X_1^2}{\partial^2 G/\partial X_1\,\partial X_3} \qquad (16)$$

According to refs. 3 and 4, eqn. (16) is the necessary condition for calculating spinodal curves in the direction V.

Inserting eqns. (9), (10) and (11) in eqn. (15), we have the following equation:

$$\begin{aligned}&(RT)^2 m(1-m) - 2RT[mC_{34}X_3X_4 + C_{12}(1-m)X_1X_2]\\&\quad + [4C_{12}C_{34} - (C_{13} - C_{23} + C_{14} + C_{24})^2]X_1X_2X_3X_4\\&\quad = 0\end{aligned} \qquad (17)$$

To simplify eqn. (17), the following notation is introduced:

$$L = (C_{13} - C_{23} - C_{14} + C_{24})^2$$

After this transformation the unknown variable T in eqn. (17) can be calculated. The temperatures of the spinodal decomposition are given by

$$\begin{aligned}RTm(1-m) &= mC_{34}X_3X_4 + (1-m)C_{12}X_1X_2\\&\quad \pm \{[mC_{34}X_3X_4 - C_{12}(1-m)X_1X_2]^2\\&\quad + m(1-m)LX_1X_2X_3X_4\}^{1/2}\end{aligned} \qquad (18)$$

6. Results and discussion

Equation (18) can be used for all quaternary systems which have the same geometry as that described in Figs. 1 and 2. The absolute values of the parameters C_{34} and C_{12} of these quaternary systems are so small that they may be neglected. The temperatures of the spinodal decomposition are then determined by L. It must be pointed out that by the calculation of the spinodal decomposition the enthalpies of mixing of all binaries are assumed to be independent of temperature.

While the interaction parameters C_{12} and C_{34} in the quaternary Fe–Ni–Ti–Zr and Fe–Co–Ti–Zr systems have small absolute values, the L values in both of the quaternary systems are large. Since a negative temperature is meaningless in this case, the minus sign in eqn. (18) may be cancelled. Because of the different signs of the parameters C_{12} and C_{34} in the Ni–Co–Ti–Zr system, the following relation holds:

$$mC_{34}X_3X_4+(1-m)C_{12}X_1X_2 < |mC_{34}X_3X_4-C_{12}(1-m)X_1X_2| \tag{19}$$

Therefore the temperatures of spinodal decomposition for all three quaternary systems considered here are given by

$$RTm(1-m)=mC_{34}X_3X_4+(1-m)C_{12}X_1X_2 +\{[mC_{34}X_3X_4-C_{12}(1-m)X_1X_2]^2 +m(1-m)LX_1X_2X_3X_4\}^{1/2} \tag{20}$$

Figure 6 shows the temperatures of the spinodal decomposition as functions of compositions X_1 and X_3 in three-dimensional figures, where the heavy lines describe isotherms. The calculations shown in Fig. 6 are carried out for the section $m=0.5$. The critical temperature of spinodal decomposition of the quaternary Fe–Ni–Ti–Zr system is approximately 850 K. While the Fe–Co–Ti–Zr system exhibits a critical temperature of 930 K, the quaternary Ni–Co–Ti–Zr system has a critical temperature of spinodal decomposition of 60 K. The low critical temperature in the Ni–Co–Ti–Zr system is attributed to the small value of L.

Figure 7(a) shows the temperature of the spinodal decomposition for the Fe–Ni–Ti–Zr system at the section $m=0.6$. As shown in Fig. 7(a), the critical temperature has decreased to 480 K. In Fig. 7(b) the temperature of the spinodal decomposition is illustrated for the Fe–Ni–Ti–Zr system at the section $m=0.7$. The critical temperature drops almost to 140 K. However, the critical temperature of the spinodal decomposition for the section $m=0.4$ increases to 1160 K, as shown in Fig. 7(c). It is seen clearly that the critical temperature of the spinodal decomposition depends strongly on the situation of the sections.

Here the conclusion can be drawn that undercooled liquid Fe–Ni–Ti–Zr and Fe–Co–Ti–Zr alloys at the section $m=0.5$ could exhibit spinodal decomposition at temperatures below approximately 900 K. According to the thermodynamic estimation, no spinodal decomposition can appear in the undercooled liquid Ni–Co–Ti–Zr alloys at the section $m=0.5$.

Acknowledgment

H. Wang is indebted to the Konrad Adenauer Foundation for a scholarship.

References

1 R. Lück, H. Wang and B. Predel, *Z. Metallkd., 82* (1991) 807.
2 H. Wang, R. Lück and B. Predel, *J. Phase Equilib.*, in press.
3 J. L. Meijering, *Philips Res. Rep., 5* (1950) 333.
4 J. L. Meijering, *Philips Res. Rep., 6* (1951) 183.
5 H. Wang, R. Lück and B. Predel, *Z. Metallkd., 82* (1991) 659.
6 H. Wang, R. Lück and B. Predel, *Z. Metallkd., 83* (1992) 528.
7 R. Lück, I. Arpshofen, B. Predel and J. F. Smith, *Thermochim. Acta, 131* (1988) 171.
8 H. Wang, R. Lück and B. Predel, *Z. Metallkd., 81* (1990) 843.
9 R. Lück, H. Wang and B. Predel, *Z. Anorg. Allg. Chem.*, in press.
10 I. Arpshofen, R. Lück, B. Predel and J. F. Smith, *J. Phase Equilib., 12* (1991) 141.
11 B. Predel and R. Mohs, *Arch. Eisenhüttenwes., 41* (1970) 143.
12 L. Kaufman and H. Bernstein, *Computer Calculation of Phase Diagrams,* Academic Press, New York, 1970.
13 R. Lück, Z. C. Wang and B. Predel, *J. Non-Cryst. Solids, 117–118* (1990) 529.
14 H. Wang, R. Lück and B. Predel, *Z. Metallkd., 82* (1991) 626.